Parallel Reaction Monitoring for High Resolution and High Mass Accuracy Quantitative, Targeted Proteomics*[S]

Amelia C. Peterson‡, Jason D. Russell‡, Derek J. Bailey‡, Michael S. Westphall‡, and Joshua J. Coon‡§

Selected reaction monitoring on a triple quadrupole mass spectrometer is currently experiencing a renaissance within the proteomics community for its, as yet, unparalleled ability to characterize and quantify a set of proteins reproducibly, completely, and with high sensitivity. Given the immense benefit that high resolution and accurate mass instruments have brought to the discovery proteomics field, we wondered if highly accurate mass measurement capabilities could be leveraged to provide benefits in the targeted proteomics domain as well. Here, we propose a new targeted proteomics paradigm centered on the use of next generation, quadrupole-equipped high resolution and accurate mass instruments: parallel reaction monitoring (PRM). In PRM, the third quadrupole of a triple quadrupole is substituted with a high resolution and accurate mass mass analyzer to permit the parallel detection of all target product ions in one, concerted high resolution mass analysis. We detail the analytical performance of the PRM method, using a quadrupole-equipped bench-top Orbitrap MS, and draw a performance comparison to selected reaction monitoring in terms of run-to-run reproducibility, dynamic range, and measurement accuracy. In addition to requiring minimal upfront method development and facilitating automated data analysis, PRM yielded quantitative data over a wider dynamic range than selected reaction monitoring in the presence of a yeast background matrix because of PRM's high selectivity in the mass-to-charge domain. With achievable linearity over the quantifiable dynamic range found to be statistically equal between the two methods, our investigation suggests that PRM will be a promising new addition to the quantitative proteomics toolbox. ***Molecular & Cellular Proteomics 11: 10.1074/mcp.O112.020131, 1475–1488, 2012.***

The most widespread protein sequencing technique is the shotgun method. Proteins are digested into peptides, chromatographically separated, and measured by mass spectrometers (1–10). Many types of mass spectrometers are used—quadrupole ion traps, quadrupole ion trap hybrids such as the QLT (quadrupole linear ion trap)-Orbitrap or QLT-FT-ICR, and quadrupole time-of-flight (Q-TOF) hybrids—but, the experiments, from the MS measurement onward, are basically identical: the masses of eluting cationic peptide precursors are measured in a MS scan, and the most abundant precursors are selected in series for successive tandem MS events (MS/MS). This process, called data-dependent acquisition, continues for the duration of a chromatographic separation, and constant MS operation in this manner can generate hundreds of thousands of spectra in days. These spectra are then mapped to peptide or protein sequence databases using highly-evolved database search algorithms (11–13). Successful results can be obtained within just a few days and are nothing short of spectacular: tens of thousands of unique peptide spectral matches mapping to several thousand unique protein isoforms have become the norm. Although this approach certainly can achieve ultra-high-throughput, it is unfortunately lacking in sensitivity and reproducibility. Specifically, complete coverage of specific biological pathways or functional groups is not typical (*i.e.* all 500 kinases, 1400 transcription factors, *etc.*). Likewise, the overlap of identifications in replicate experiments is low (35–60%) (14, 15).

The limitations of the shotgun method have propelled a recent fervor in targeted proteomic methods—namely, selected reaction monitoring (SRM[1], also known as MRM, multiple reaction monitoring) (16–21). SRM achieves the reproducibility and sensitivity that the shotgun approach lacks, and even offers a route to determine absolute abundance (21). By offering superior consistency, completeness, and quantitative accuracy, targeted experiments afford a new avenue to test and generate biological hypotheses (15). SRM, primarily per-

From the ‡Departments of Chemistry and Biomolecular Chemistry, and Genome Center of Wisconsin, University of Wisconsin – Madison, Madison, Wisconsin 53706

Received April 28, 2012, and in revised form, August 2, 2012
Published, MCP Papers in Press, August 3, 2012, DOI 10.1074/mcp.O112.020131

[1] The abbreviations used are: PRM, parallel reaction monitoring; SIM, selected ion monitoring; MRM, multiple reaction monitoring; SRM, selected reaction monitoring; QqQ, triple quadrupole; QqOrbi, quadrupole-quadrupole Orbitrap; QqTOF, quadrupole-quadrupole time-of-flight; HR/AM, high resolution/accurate mass; CAD, collisionally activated dissociation; HCD, higher energy c-trap dissociation; RSD, relative standard deviation; XSC, extracted score chromatogram; XIC, extracted ion chromatogram; AUC, area-under-the-curve.

formed on triple quadrupole (QqQ) MS, has emerged as the MS "gold-standard" for targeted proteomics (21) and is a broadly accepted alternative to the traditional multiplexed immunoassay (20). Numerous studies have successfully employed QqQ SRM for both absolute and relative quantitation of analytes in applications ranging from clinical diagnostics (22–27) to whole systems analyses (28–30). The rising popularity and promise of the SRM technique have also spawned a plethora of new analysis approaches and software tools. For example, many algorithms and software tools have been developed to expedite assay development by aiding in the selection of proteotypic peptides (31), peptide transitions, and instrument parameters (reviewed in Cham Mead *et al.* (32)). Additionally, through community effort, several publicly available databases of tandem MS spectra (33–39) and validated SRM assays (40, 41) are available to provide empirical guides to transition selection and assay development. Several groups have also presented elegant solutions to maximize instrument duty cycle and improve assay specificity. Picotti and colleagues (42), for instance, demonstrated use of synthetic peptide libraries to accelerate SRM assay development. Likewise, Kiyonami *et al.* (43) recently introduced a strategy that boosted SRM bandwidth by restricting the number of transitions per target acquired before and after target elution. By limiting the acquisition of full transition sets to a few occasions during peptide elution, this strategy enabled simultaneous qualitative and quantitative analysis of 6000 transitions in one hour, a substantial boon to SRM throughput.

In recent years, discovery-based proteomic methods, such as the shotgun method discussed above, have been transformed by significant advancements in instrumentation; key figures of merit, such as sensitivity, duty cycle, mass accuracy, and mass resolution have seen remarkable improvements (44). Although these developments have done little to directly curtail the reproducibility issues that the SRM method so effectively counters, the achievable depth of proteomic sampling (*i.e.* analytical sensitivity) within the discovery context continues to improve. Central to this evolution is the increased performance, and availability, of high resolution and accurate mass (HR/AM) instrumentation (44). Namely, developments in time-of-flight (TOF) technology (45), and the advent of the Orbitrap mass analyzer in 2005 (46–49), have made fast and sensitive MS/MS scanning (50–53) with $<$10 parts-per-million (ppm) mass measurement error routine (54). For discovery experiments, the ability to acquire MS/MS scans with high resolution and low-ppm mass errors offers several advantages, including higher confidence sequence identification (44, 55), post-translational modification site localization (56), and improved quantitative accuracy. Coming from this perspective, we wondered whether the highly accurate mass measurement capabilities of today's new-generation MS instrumentation could be leveraged to provide benefits within the targeted proteomics domain.

Driving our inquiry was the newly introduced Q Exactive bench-top quadrupole-Orbitrap MS (QqOrbi) (47), which, along with quadrupole-TOF (QqTOF) instrumentation (45), possesses a geometry essentially equivalent to a QqQ, except that the third quadrupole of the QqQ is replaced by an Orbitrap (or TOF) analyzer (Fig. 1*A*, 1*B*). The QqOrbi achieves a 12 Hz scan rate at a resolution of 17,500 for both MS and MS/MS scanning, quadrupole mass filter isolation with mass windows as small as $\pm$0.2 Th, and mass measurement errors typically $<$1 ppm with internal calibration and $<$5 ppm with external calibration (47). With these performance characteristics, we envisioned a targeted proteomics strategy where all products of a target peptide are simultaneously monitored under conditions that offer high resolution and high mass accuracy. Operation would be identical to a SRM scan except that all transitions would be codetected and distinguished from one another, and from background, by the final mass analysis stage. We call this mode of operation parallel reaction monitoring (PRM).

The PRM technique has several potential advantages over the traditional SRM approach. First, PRM spectra would be highly specific because all potential product ions of a peptide, instead of just 3–5 transitions, are available to confirm the identity of the peptide (57, 58). Second, PRM could provide a higher tolerance for co-isolated background peptides/species. Because numerous ions would be available for identification and quantitation purposes, the presence of interfering ions in a full mass spectrum would be less disruptive to overall spectral quality than interference in a narrow mass range, especially because high resolution can often separate these ions from the product of interest. Note that one could extend this concept to a multiplexed PRM scan where the product ions of several target peptides are comingled and detected in a single-scan (47). And third, because PRM monitors all transitions, one need not have prior knowledge of, or preselect, target transitions before analysis. These points suggest another potential advantage of the PRM approach: elimination of much of the effort required to develop and optimize the traditional SRM assay.

Given that a QqQ possesses a duty cycle approaching 100% and uses electron multiplier-based detection, which is inherently more sensitive than image current-based detection (Orbitrap), it is not obvious that the PRM method will afford sensitivity comparable to the current state-of-the-art SRM approach. However, we postulate that what PRM lacks in sensitivity and duty cycle might be effectively countered by the selectivity of HR/AM measurement. Here, we implement PRM on a QqOrbi system and benchmark method performance with triplicate analysis of 25 isotopically heavy-labeled synthetic peptides spanning a concentration range of 10^5 under neat and matrix-containing conditions. We assess key figures of merit, including data quality, run-to-run reproducibility/precision, dynamic range/sensitivity, and measurement

accuracy/linearity. Finally, we draw a performance comparison to SRM operating on a common QqQ platform.

EXPERIMENTAL PROCEDURES

Materials and Reagents—Unless otherwise specified, all reagents used herein were purchased from Sigma Aldrich (St. Louis, MO). Acetonitrile was purchased from Fisher Scientific (Fair Lawn, NJ) and formic acid (>99%) from Thermo Fisher Scientific (TFS, Rockford, IL). Ultrapure water was supplied from a Barnstead Nanopure Diamond ultrapure water system (resistivity 18.2 MΩ-cm; TFS, Dubuque, Iowa).

Sample Preparation—Twenty-five heavy-labeled hypothetical tryptic human peptides (Table I) were synthesized by Fmoc solid-phase synthesis, purified by HPLC, and solubilized in 5% v/v CH_3CN/water at a concentration of 5 pmol/μl ± 25% with purity >97% (Heavy-Peptides AQUA QuantPro; TFS, Ulm, Germany). All 25 peptides (QqOrbi experiments) or a selection of 14 of the 25 peptides (QqQ experiments) were mixed and used neat with intact bovine serum albumin (BSA) carrier protein (200 fmol/μl in 0.1% HCOOH/water) or spiked into a whole-cell tryptic digest of yeast (1 μg/μl in 0.1% HCOOH/water), prepared as previously reported (59), at the following concentrations (fmol/μl or nM): 0.002, 0.02, 0.2, 2, 20, and 200. A one microliter aliquot of each sample was subjected to C_{18}-reversed phase liquid chromatography prior to mass spectrometry (see supplemental Methods 1.1 for liquid chromatography conditions).

Mass Spectrometry—In all experiments, HPLC eluent was introduced into the mass spectrometer via an integrated electrospray emitter (60) (pulled in-house via laser micropipette puller; Sutter Instrument, Novato, CA) operated at 2.0–2.2 kV and coupled to a custom nano-ESI source. QqOrbi experiments were performed on a quadrupole mass filter-equipped bench-top Orbitrap mass spectrometer (Q Exactive, TFS, Bremen, Germany). Each sample (6 concentrations × 2 background matrix conditions) was analyzed in triplicate under two mass spectrometric conditions: 1) PRM with an isolation width of ±1 Th, and 2) PRM with an isolation width of ±0.2 Th. Samples were analyzed in order of increasing concentration with an extensive column wash between each concentration set to minimize carry-over. In all experiments, a full mass spectrum at 70,000 resolution relative to *m/z* 200 (AGC target 1×10^6, 250 ms maximum injection time, *m/z* 200–2000) was followed by up to 25 PRM scans at 17500 resolution (AGC target 2×10^5, 120 ms maximum injection time) as triggered by a scheduled inclusion list (Table I). Ion activation/dissociation was performed by beam-type CAD at a normalized collision energy of 25% in a higher-energy c-trap dissociation (HCD) collision cell. Instrument spectral mass accuracy was checked and calibrated after each concentration set (approximately every 1.5 days). PRM parameters were optimized and selected from prior experiments (supplemental Results and Discussion 2.1 and supplemental Fig. S6).

QqQ experiments were performed on a TSQ Quantum Discovery Max (TFS, Austin, TX). Each sample was analyzed in triplicate in order of increasing concentration, targeting a selected set of 14 peptides in scheduled SRM mode (see Table I for transitions, collision energies, and scheduling). For each transition, a 35 ms dwell time, Q1 and Q3 selectivities of 1.0 and 0.7 Th (FWHM), respectively, and Q2 collision gas pressure of 1.0 mTorr argon were employed. Collision energies (CE) for each peptide precursor were individually optimized in prior experiments (data not shown) using the following empirically derived formula as a reference point: CE = 0.025 x precursor *m/z* + 12.

Data Analysis—PRM data were manually curated within Xcalibur Qual Browser (version 2.2.0.23; TFS, San Jose, CA) and through use of an internally developed script, ElutionProfiler. Elution Profiler was developed in C#/.NET with Microsoft Visual Studio 2010 and .NET Framework version 3.5 (Redmond, WA) (available on our website at http://www.chem.wisc.edu/~coon/software.php). Access to data in the proprietary TFS .raw file format was enabled by the XRawfile Component Object Model (COM) library (XRawfile2.dll, installed automatically with Thermo Xcalibur). ElutionProfiler used .raw files as input to generate an extracted score chromatogram (XSC) for each PRM spectrum. The spectral score was calculated based on all present, sequence-specific *b*- and *y*-ions using the following formula (Eq. 1):

$$Score = \sum_{n}^{k}(0.25\delta_b(n) + \delta_y(n))n$$

where the result of the Dirac delta functions, δ_b and δ_y, is 1 if the *n*th ion in the spectrum is a *b*- or *y*-ion with <5 ppm mass error, respectively, and 0 in all other cases. *n* is the product ion number (*e.g.* 4 for a y_4 or b_4 ion), *k* is the length of the peptide (number of amino acids), and 0.25 is an arbitrarily-chosen scalar to weight *b*-ions (not containing an isotopically heavy-labeled arginine or lysine at the c-terminus) less than equivalently numbered *y*-ions. XICs were generated using the summed intensity of all possible *b*- and *y*-product ions for a particular peptide, extracted at a ±10 ppm mass tolerance. Detection was based on the presence of product ion signals in at least 2 of 3 replicates within $\pm 3\sigma$ min of the expected retention time, mass error within ±5 ppm, chromatographic signal-to-noise ≥3, and the presence of a combination of product ions in at least one spectrum with a score meeting or exceeding a peptide-specific threshold equal to the length of the targeted peptide (*k*) in all cases. See supplemental Methods 1.2 for QqQ SRM detection criteria, calculation of performance metrics, and statistical methods.

In Silico Calculations—A script, available at http://www.chem.wisc.edu/~coon/software.php, was written in C#/.NET using Visual Studio 2010 for all *in silico* calculations referenced in the text. The human tryptic peptidome was modeled using the UniProtKB human protein database (accessed 11 Nov 2011, http://www.uniprot.org/taxonomy/complete-proteomes) with the following parameters: ≥1 enzyme terminus, ≤4 missed cleavages, peptide length of 5–45 amino acids, intact peptide mass of 200–9000 Da, fixed cysteine carbamidomethylation, variable methionine oxidation, and assumed cleavage of initiator methionine residues. Each of the 20,332,717 unique peptide sequences comprising the human peptidome was assessed for its potential to interfere in precursor and product ion measurement of the 25 peptide sequences studied here, in both light and heavy forms (50 total), considering the *y*-ion transitions monitored on the QqQ (Table I). For peptides not monitored on the QqQ, equivalent *y*-ions were chosen. Intact confounder peptides were considered in charge states from 1–5 (monoisotopic mass only, isotopes were not considered). Confounder product ions were considered in charge states from 1 to one less the precursor charge state and were of the following ion types: *b*, *y*, *a*, *b/y/a* - H_2O if containing amino acids D, E, S, or T, *b/y/a* - NH_3 if containing amino acids K, N, Q, or R, internal fragments, and sequence-specific immonium ions. Interference in all QqOrbi examples met the following requirements: mass measurement tolerance of ±5 ppm and precursor isolation width of ±1 Th. Interference in all QqQ examples met the following requirements: mass measurement tolerance of ±250 ppm, precursor isolation width (Q1) of ±0.5 Th, and product isolation width (Q3) of ±0.35 Th.

All data referenced in this study is available as Thermo .raw files at http://www.chem.wisc.edu/~coon/Downloads/RawData/Peterson_PRM_QqOrbi.zip/ and /Peterson_PRM_QqQ.zip/.

RESULTS AND DISCUSSION

Here, we investigate the performance of parallel reaction monitoring (PRM) on a high resolution and accurate mass (HR/AM) quadrupole-Orbitrap mass spectrometer (QqOrbi) for targeted, quantitative proteomics with respect to the gold-

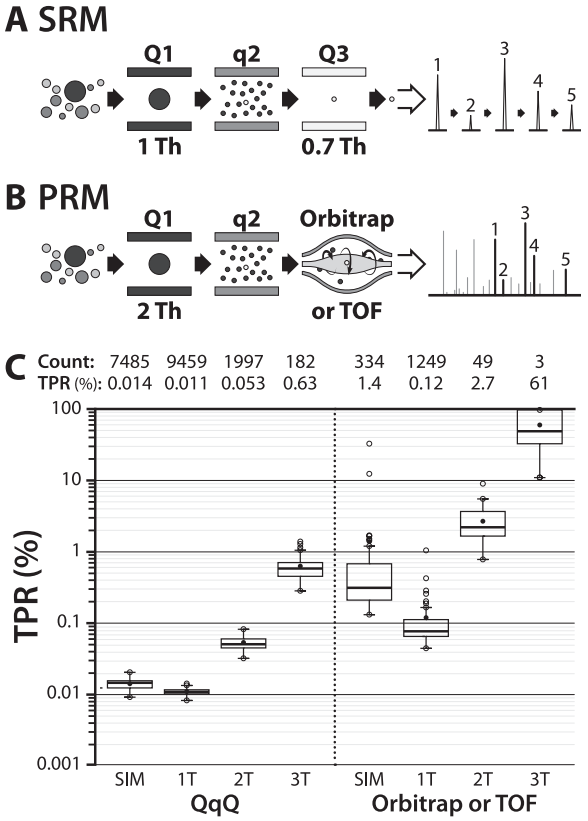

FIG. 1. **Schematic representation of SRM (*A*) and PRM (*B*) as performed on QqQ and QqOrbi (or QqTOF) instrumentation, respectively.** In SRM (*A*), each product ion transition (white circle) is serially monitored (from 1 to 5) one at a time in distinct scans. In PRM (*B*), all product ion transitions (1–5, and all possible product ions, shown as black circles) are analyzed/monitored in one concerted, high resolution and high mass accuracy mass analysis. Q1 and Q3 refer to the first and third mass-resolving quadrupoles of the QqOrbi (Q1 only) and QqQ, and q2 to the quadrupole (or cell, in the QqOrbi case) in which beam-type CAD is performed. The isolation widths employed for each device in both experimental and theoretical data are given below each respective device. *C*, Theoretical comparison of the rate of correctly identifying a target peptide (as true positive rate in percent, TPR) from all theoretically possible peptides in the human tryptic peptidome in SIM and reaction monitoring experiments in which 1, 2, and 3 *y*-ion transitions (labeled as 1T, 2T, and 3T, respectively) are monitored for Orbitrap or TOF instruments (±5 ppm) and QqQ (±250 ppm) for the 25 peptides used in this study in their light and heavy forms (50 total peptides). Count refers to the average number of possible confounding species, including the target peptide, represented by the boxplots. TPR is calculated as 100/count.

standard SRM method performed on a triple quadrupole (QqQ) instrument. In PRM, we have substituted a HR/AM Orbitrap mass analyzer for Q3 within the context of a conventional SRM experiment. Thus, instead of *serially* monitoring target transitions over several ion injections and low resolution mass measurement periods (Fig. 1*A*), PRM monitors all product ions of a mass-selected peptide target *in parallel* with one ion injection and full mass range Orbitrap mass analysis (Fig. 1*B*). We queried a set of 25 isotopically heavy-labeled synthetic peptides spanning six orders-of-magnitude in concentration (2 pM to 200 nM, corresponding to 2 amol to 200 fmol on column) with and without peptide background using PRM with isolation widths of ±1 and ±0.2 Th. Three technical replicates were performed for each experiment with one microliter of sample injected on column in all experiments. For comparison, we analyzed 14 of the 25 peptides using a traditional, optimized QqQ SRM assay. Equivalent experiments and comparisons were also performed using selected ion monitoring (SIM) on the QqOrbi. Although not described in the body text in detail, interested readers can consult the supplemental Results and Discussion 2.4–2.6 and supplemental Fig. S5 for more information.

Theoretical Comparison of SRM and PRM—The process of targeting a peptide with SRM involves two stages of quadrupole mass filtering with tight tolerances for both members of a precursor-product ion transition. Because all product ion transitions targeted for a given precursor peptide (usually 3 to 5) are required to simultaneously elute, the likelihood of mistaking a nontarget peptide or background ion for the targeted peptide is a rare occurrence; hence, SRM is considered to be a highly specific assay. The proposed PRM method involves only *one* stage of quadrupole mass filtering (of the precursor of interest) before mass analysis in an Orbitrap. The Orbitrap, however, by nature of its high resolution and high mass accuracy should more effectively separate ions of interest from background ions than the electron multiplier-based detection used in a QqQ. Thus, to motivate our experiments, we asked how PRM compares theoretically to SRM in terms of specificity. In other words, can the selectivity of Orbitrap HR/AM mass analysis make up for use of only one stage of mass filtering?

To answer this question, we digested the human proteome with trypsin *in silico* to yield over 20 million unique peptide sequences (see Experimental Procedures for details). For our calculations, we considered these peptides to be potential confounders in the measurement of the precursor and product ions of the 25 isotopically heavy-labeled peptides targeted in this study, as well as their 25 corresponding unlabeled peptides (50 total). For each unique confounder peptide, considered in charge states from 1 to 5, we further generated all possible *b*, *y*, *a*, *b*/*y*/*a* - water, and *b*/*y*/*a* - ammonia product ions, internal fragments, and immonium ions in charges ranging from 1 to one less the precursor charge state. We then asked how often, depending on the amount of evidence required by the assay and the mass analyzer employed, the numerous ions generated by the confounder population resulted in indistinguishable interference in the measurement of one of our target peptides. The results of these queries are summarized in Fig. 1*C*.

First, we consider a query requiring the least evidence of the targeted peptide, a SIM experiment. In SIM, an intact target peptide ion is isolated in Q1 and mass analyzed without further transformation. We begin our theoretical calculations with SIM to explore the effect of mass accuracy/resolution

alone on selectivity. Assuming Q1 isolation widths of ±0.5 and 1 Th, and mass errors less than ±250 and 5 ppm, for the QqQ and QqOrbi, respectively, highly accurate mass analysis improves the chances of correctly identifying the target peptide (96 ± 3%) by exclusion of a large number of spurious peptides (7151 ± 1447, on average). Still, such an experiment, however, would only produce an unambiguous identification ~1% of the time (Fig. 1*C*). Note, these calculations assume no upfront chromatographic separations and that all genome-predicted peptides are translated and detectable (*i.e.* the worst-case scenario).

Though it is obvious that high accuracy mass measurements increase specificity, it is less clear that this benefit persists in reaction monitoring experiments. To test this, we considered the number of intact peptides that could potentially be co-isolated with a given target peptide (assuming ±1 and ±0.5 Th Q1 isolation windows centered on the target peptide *m/z* for the QqOrbi and QqQ, respectively) and then generate at least one product ion (of any type) with a *m/z* within ±5 ppm (QqOrbi) or ±250 ppm (QqQ) of a *y*-ion transition from the target peptide. As shown in Fig. 1*C*, the specificity of a HR/AM analyzer substantially reduces the number of spurious peptide ions that can interfere in the correct identification of a target peptide by its *y*-ion transitions (shown as the rate of correct target identification, or true positive rate). The inclusion of 1, 2, or 3 *y*-ion transitions with high mass accuracy measurement results in approximately a (10 ± 14)-fold, (53 ± 35)-fold, and (112 ± 81)-fold greater likelihood of correctly identifying a target peptide compared with the inclusion of 1, 2, or 3 *y*-ion transitions at low resolution, respectively. Even if observation of all three *y*-ion transitions were required, as is typically the case in QqQ SRM assays, the likelihood of correctly identifying a target at low resolution and unit mass accuracy is still less than 1% for the 50 peptides considered here (0.6 ± 0.3%). Again, these calculations do not consider the significant benefit that is achieved by chromatographic separation and model a worst-case scenario. Even still, the detection of three *y*-ion transitions at high mass accuracy (*i.e.* <5 ppm mass error) provides nearly unambiguous target confirmation (1.6 ± 1.1 potential confounders) from the background of the entire human peptidome.

These theoretical calculations confirm our guiding supposition that PRM can provide greater routine specificity as compared with conventional SRM. Whether this result implies greater overall performance in targeted, quantitative proteomics studies compared with SRM, however, depends on several additional, but important, factors: whether both analyzers, one image current-based and the other electron multiplier-based, are capable of detecting the targeted species, and whether both analyzers can reproducibly *and* accurately measure the abundance of the targeted species. Given that PRM relies on an analyzer that is fundamentally less sensitive and slower than that used in SRM, investigation of these factors will reveal whether selectivity/specificity can overcome limitations in speed and sensitivity. In the following sections, we empirically investigate this issue through a systematic analysis of reproducibility, sensitivity, and linearity of both methods.

Detection Criteria for PRM and SRM—The detection criteria we developed for PRM incorporate the benefits of high selectivity and specificity HR/AM mass analysis, as discussed above. By making use of full mass range MS/MS spectra and the high specificity of product ions when measured with high mass accuracy, we developed an automated detection algorithm that assigned a spectral score to each PRM spectrum based on the presence of *b*- or *y*-ions within ±5 ppm of expected target-specific product ions using Eq. 1, and then generated an "extracted score chromatogram" (XSC) for that peptide. In the design of our spectral score, we chose to weight *b*-ions less than equivalently numbered *y*-ions because all of the peptides targeted in this study were isotopically heavy-labeled at the c-terminus and analyzed in a background of endogenous yeast peptides. Thus, *y*-ions, containing the heavy label, were more specific to our target peptides than *b*-ions and were weighted as such. If the target peptides of interest were not heavy-labeled, one might consider equally weighting *b*- and *y*-ions for scoring purposes. A positive detection event required that, in at least 2 of 3 replicates, the XSC met or exceeded a peptide specific threshold (equal to the length of the target peptide) within $\pm 3\sigma$ min of the expected retention time (supplemental Fig. S1). Fig. 2 shows the application of this score to exemplary data from the peptide AETLVQAr (#17) under neat and matrix-containing conditions over all six peptide concentrations. The XSCs (gray) are overlaid with XICs (blue) generated using the summed intensity of all *b*- and *y*-ions present in each spectrum. Note that XSCs are used solely for establishing a detection event and not for quantification as the score is independent of ion intensity. Following a positive detection event, the target-specific ions that generated the detection event are extracted as an XIC for quantification. This peptide was detected at concentrations spanning four orders-of-magnitude (from 20 pM to 200 nM) without matrix, and over three orders-of-magnitude (from 200 pM to 200 nM) in the presence of yeast matrix.

In Fig. 2, at high target peptide concentrations (*e.g.* 20–200 nM), the XSC often increases above threshold before the XIC shows any noticeable intensity change and stays above threshold after the XIC intensity has fallen. This characteristic is ascribable to the intensity-independence of the score, and suggests that high quality Orbitrap spectra, in terms of the presence of product ions with high mass accuracy, can be acquired independently of ion intensity above some intensity threshold. At low concentration, especially in the presence of matrix (see 200 pM in matrix), the XSC easily distinguishes nearby, spurious XIC signals from target-derived signals, demonstrating score specificity. The detection threshold was

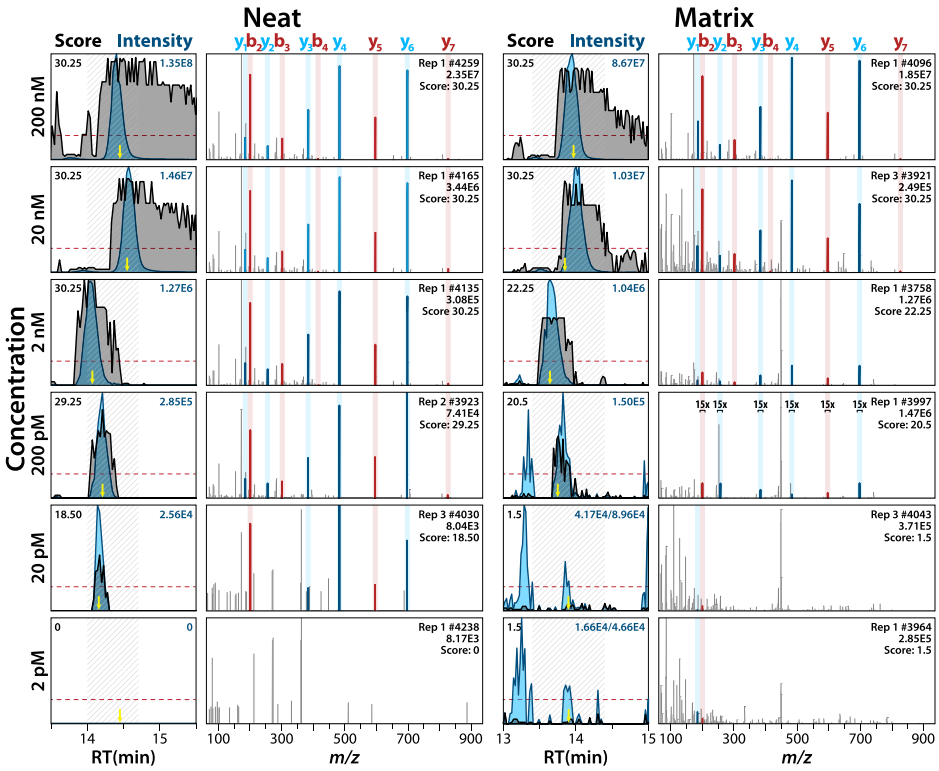

FIG. 2. **Extracted PRM score chromatograms (XSC, ±5 ppm, gray) overlaid with XICs (±5 ppm, blue; 7-point boxcar smoothed) and single-scan PRM spectra for peptide AETLVQAr (#17) isolated at ±1 Th under neat (*left*) and matrix-containing (*right*) conditions from 2 pM to 200 nM.** *Red dotted line* in XSC plots represents the score acceptance threshold (8) for this peptide. Product ions detected in each spectrum are *highlighted* and the spectral score is labeled. *Yellow arrows* in each XIC/XSC plot indicate the retention time at which the associated single-scan spectrum was acquired. *Hashed area* in XIC/XSC plots designates the retention time period during which peak elution was expected based on the $\pm 3\sigma$ range around the average retention time observed in 200 nM analyses.

chosen to ensure that an accepted score (signifying target detection) would, at least, contain one *y*-ion with *m/z* greater than the precursor *m/z*. Although this threshold does not definitively ensure that a score above the threshold is entirely specific to only the target peptide, use of the threshold successfully separated spurious signals from target-specific signals, agreeing with or being more conservative than manual interpretation of the data in all cases. supplemental Fig. S2 plots the distribution of the spectral score for all possible combinations of *b*- and *y*-ions arising from an eight-amino-acid peptide, such as AETLVQAr, by the fraction of the score described by each ion. Example ion combinations are given at several scores below and above the threshold. supplemental Table S1*A–D* catalog the maximum XSC scores measured for each replicate, concentration, and PRM experiment type (supplemental Results and Discussion 2.2).

QqQ SRM experiments were performed to provide a standard for comparison of our QqOrbi PRM data. QqQ SRM data were analyzed manually based on detection criteria commonly used in the literature for SRM analyses (42). A positive peptide detection event occurred when eight of 10 criteria were met in a least two of three replicates. Originally, we required 10 of 10 criteria to be met in at least two of three replicates, but relaxed this criterion to improve the completeness of the data set and thus our ability to compare it to the PRM data set. The ten criteria were: 1) the appearance of three co-eluting transitions within ±2.5 min of the expected retention time (supplemental Fig. S1), 2–4) average transition *m/z* within ±500 ppm of the expected *m/z*, 5–7) average transition abundance within ±15% of the expected abundance, and 8–10) individual transition XICs with signal-to-noise meeting or exceeding three. Peptides, transitions, and other experimental parameters for SRM are listed in Table I.

Fig. 3*A* compares PRM with ±1 Th isolation to SRM for the detection of peptide GVSAFSTWEk (#1) at 200 pM and 2 nM (200 amol and 2 fmol, respectively, on column) in the presence of yeast matrix. In PRM, the signals present in the XIC during the entire duration for which this peptide was targeted are exclusively due to the targeted peptide, even at the lowest concentration detected (200 pM; XICs at lower concentrations had zero intensity). Numerous other *y*-ions (shown in gray) are also present at the 2 nM level, adding confidence to the detection and generating maximum spectral scores well above the threshold of 10 for this peptide. By contrast, transition XICs in the SRM data show numerous background signals throughout the duration over which the peptide was targeted (far right). At the 200 pM level, while numerous signals are present in the XICs for each SRM transition, the high level of chemical noise in all transition

TABLE I
Peptides and instrument parameters used in this study

c - carbamidomethylcysteine (+ C_2H_3NO), **r** - heavy labeled arginine ($^{13}C_6{}^{15}N_4$), **k** - heavy labeled lysine ($^{13}C_6{}^{15}N_2$).

#	Peptide[a]	PRM parameters			SRM parameters			
		Mono. mass	Parent *m/z*	Sched. RT (min)	Parent *m/z*	Transition *m/z*	CE (%)	Sched. RT (min)
1	GVSAFSTWE**k**	1118.5488	560.2817	28.0–33.0	560.584	658.646 805.821 963.977	26	35.0–89.0
2	HFLTLAPI**k**	1046.6368	524.3257	26.5–31.0				
3	ARPA**c**VDA**r**	1024.5112	513.2653	0.0–10.0				
4	SGWT**c**TQPGG**r**	1281.5753	608.7738	13.0–20.0				
5	EGQLAAGT**c**EIVTLD**r**	1741.8544	871.9345	29.0–36.0	872.432	1174.245 1245.323 1316.402	30	37.5–89.0
6	LWSLAEIATSDL**k**	1476.5364	727.9027	40.0–53.0				
7	SEDEDEDEGDAT**r**	1648.8118	739.2755	7.0–14.0				
8	DIQFGSQI**k**	1042.5539	522.2842	23.0–29.0	522.557	540.555 687.731 815.861	25	29.0–37.5
9	HTGTPLGDIPYG**k**	1436.6875	682.3584	22.5–27.0				
10	NSWGTDWGE**k**	1215.5330	594.2640	25.5–30.5	594.580	743.708 800.760 986.971	27	29.0–37.5
11	FSDLTEEEF**r**	1362.7023	641.7949	27.0–31.5	642.134	719.675 820.762 933.920	28	29.0–89.0
12	SFEGTDYG**k**	1010.4436	506.2291	13.0–20.0	506.491	591.556 648.608 777.723	25	22.0–29.0
13	TLNGIQLA**r**	994.5799	498.2972	21.0–26.5	498.544	610.663 667.715 781.818	26	22.0–35.0
14	AFSQNSVLI**k**	1113.6274	557.8210	22.5–27.0				
15	WPGYLNGG**r**	1028.5067	515.2606	26.5–31.0	515.532	689.677 746.729 843.845	25	29.0–89.0
16	GALDGEAP**r**	894.4435	448.2290	10.0–20.0	448.441	539.498 654.586 767.745	23	1.0–29.0
17	AETLVQA**r**	896.4955	449.2550	10.0–20.0	449.471	483.478 596.636 697.741	23	1.0–29.0
18	FLNPEW**k**	940.4898	471.2522	26.5–31.0				
19	LEQNPEESQDI**k**	1453.7908	719.3510	10.0–20.0				
20	SEASSSPPVVTSSSHS**r**	1186.5135	571.2756	10.0–15.0	571.569	583.511 771.693 870.825	26	1.0–22.0
21	AP**c**QAGDL**r**	996.4686	499.2416	10.0–15.0	499.520	541.514 669.644 829.839	24	1.0–22.0
22	TWFQNQ**r**	988.4754	495.2450	20.0–26.0				
23	TVFSSTQL**c**VLND**r**	1710.8048	825.4132	31.0–40.0	825.891	899.973 1129.207 1216.285	29	37.5–89.0
24	FSEVSAD**k**	889.4273	445.7209	10.0–17.0	445.944	527.513 656.628 746.706	22	1.0–29.0
25	GLYEGTG**r**	861.4220	431.7183	10.0–20.0				

[a] All peptides have a charge state (z) of +2, except for peptide #20 (z = +3).

channels prevents confident determination of the presence of the target peptide. This example demonstrates the enhancement of sensitivity that can be achieved via PRM because of the high selectivity of HR/AM mass analysis, as well as the ease with which determinations of presence or absence of a peptide target can be made with HR/AM data.

PRM Measurement Precision—In quantitative studies, high measurement precision is critical to reliably distinguish differences between two analyses or samples. We assessed the degree of measurement precision for the PRM method, defined here as run-to-run area-under-the-curve (AUC) repeatability across technical replicates, for all concentrations and

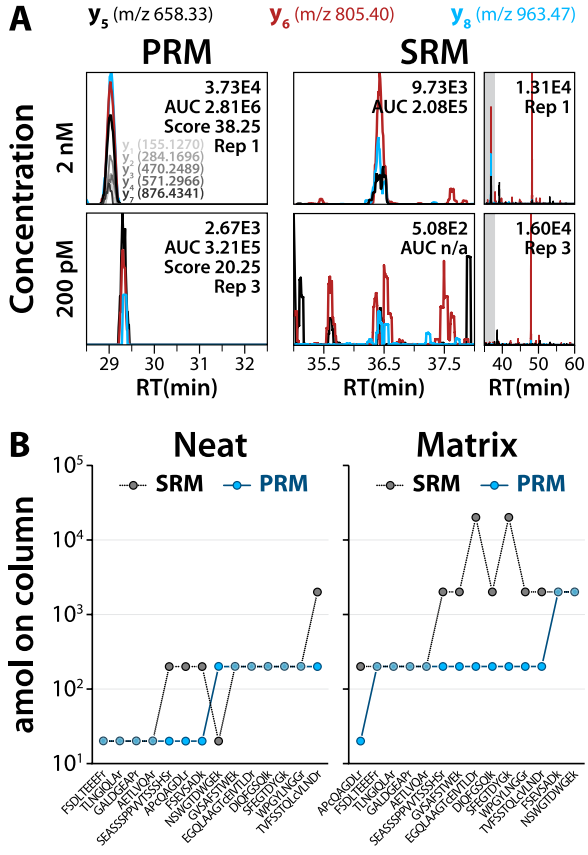

FIG. 3. ***A*, Comparison of QqOrbi PRM detection at ±1 Th with QqQ SRM for peptide GVSAFSTWEk (#1) at 200 pM and 2 nM in the presence of matrix.** Transition XICs are shown for the entire duration over which the peptide was targeted, with a zoom-in on the relevant time period in the QqQ SRM case (from the region shaded in gray in the chromatograms at the far right). Additional *y*-type product ions present in the PRM data are shown in *gray*. XICs were extracted at ±5 and ±250 ppm for PRM and SRM, respectively. The maximum spectral score attained at each concentration in PRM is also labeled. *B*, Lowest concentration detected (as number of attomoles of peptide on column) for each peptide in neat and matrix-containing experiments for the 14 peptides targeted in both SRM and PRM.

isolation widths. Overall, PRM exhibited high measurement precision with median percent relative standard deviation (%RSD) less than 10% in most cases (supplemental Table S2*A*). The main factors negatively affecting measurement precision (increasing %RSD) were low target peptide concentrations and individual peptide characteristics. Neither isolation width nor the presence of matrix resulted in statistically significant differences in precision ($\alpha = 0.05$; NB, all discussion of mean %RSDs and statistical significance refer to log-transformed data; see supplemental Methods 1.2). The precision of measurements at the lowest concentration typically detected in neat PRM, 200 pM, was significantly lower than at all other (higher) concentrations. In the matrix-containing PRM data, however, no significant differences in the measurement precision of adjacent concentrations were observed (supplemental Table S2*B*). When grouped by peptide alone, only very hydrophilic, poorly retained peptides, #3 and #7, had significantly decreased measurement precision when compared with the other 23 peptides (supplemental Table S2*C*).

We find that PRM measurement precision is consistent with studies reporting run-to-run precision data in QqQ SRM experiments. For example, in the 2009 multi-laboratory study of SRM measurement repeatability and reproducibility for peptides spiked into plasma, Addona *et al.* (20) found both intra- and inter-laboratory precision to be similarly less than 15% RSD across the concentration range studied (1–500 nM). Likewise, precision improved for measurements at higher target concentrations. Kiyonami and colleagues (43) also reported similar precision metrics in their large-scale intelligent-SRM (iSRM) experiments, observing that 80% of the 757 peptides targeted in yeast exhibited less than 10% RSD. Compared with other studies using HR/AM mass spectrometers (quadrupole linear ion trap (QLT)-Orbitrap, QqTOF, and QLT-FT-ICR) for targeted, quantitative measurements (61–65), QqOrbi PRM achieved, on average, two- to threefold better run-to-run measurement precision.

PRM Dynamic Range—On average, PRM experiments yielded quantitative information between 2–4 concentration orders-of-magnitude (93%), with the majority of experiments resulting in quantification across 3 orders-of-magnitude (54%, 0.2 to 200 nM; supplemental Table S3*A*, supplemental Fig. S3). The wider PRM isolation width, ±1 *versus* ±0.2 Th, resulted in improved dynamic range—neat, $10^{3.3}$ *versus* $10^{2.6}$, and matrix, $10^{2.7}$ *versus* $10^{2.2}$ (supplemental Table S3*B*). The presence of matrix in PRM experiments resulted in a modest depression of the quantifiable dynamic range, ~0.5 orders-of-magnitude (matrix *versus* neat, $10^{2.4}$ *versus* $10^{3.0}$). Although tighter isolation widths slightly mitigated the effects of matrix-induced sensitivity depression, at the expense of overall sensitivity, this difference was not significant (supplemental Table S3*A*). These results indicate that, although an increase in selectivity due to gas-phase enrichment would be expected by tighter isolation widths, the concomitant decrease in ion transmission at very tight isolation widths (±0.2 Th), in conjunction with Orbitrap detection, results in decreased sensitivity as too few ions are present for the target signal to exceed the Orbitrap's thermal noise band. However, with a HR/AM analyzer, the wider isolation width, which provides greater ion transmission, but also higher levels of chemical noise, can be used without a decrease in performance because of the high selectivity of the mass analysis.

Linearity of PRM Measurement Response—The linearity of measurement response—or, measurement accuracy—was calculated as the percent RSD of response factors (AUC normalized by concentration) over the concentration range for which a peptide was detected. In general, linearity was not significantly influenced by isolation width or the presence of matrix: mean neat %RSDs of 37.1 and 36.4, and mean matrix %RSDs of 35.7 and 34.2, were observed in PRM experiments with ±0.2 and ±1 Th isolation widths,

respectively (supplemental Tables S4*A*, S4*B*). If the lowest detected concentration, associated with lower overall measurement precision (*vide supra*), was excluded from each experiment, however, linearity improved and some significant differences emerged based on the presence of matrix (supplemental Tables S4*C*–S4*F*). Surprisingly, matrix-containing experiments were found to possess greater linearity than their neat counterparts in all experiments, with %RSDs of 23.2% for neat PRM and 12.0% for matrix PRM (supplemental Table S4*D*).

Because of the truncation of the measured dynamic range observed in the presence of matrix, we posited that greater linearity in matrix-containing experiments was an artifact of simply considering a smaller concentration range. Since lower precision on lower concentration measurements make it more challenging to arrive at an accurate average AUC from only three replicates, experiments quantifying over a wide dynamic range (*e.g.* neat experiments) could have decreased linearity due to low measurement accuracy at the lowest detected concentrations. To address this, we calculated an adjusted %RSD for each experiment and peptide that accounted for the dynamic range represented by a %RSD value (see supplemental Methods 1.2). The adjusted %RSD separates out contributions of dynamic range and concentration from the linearity estimate, thereby providing a more fair comparison between experiments where the dynamic range quantified is drastically different. These adjusted linearity values no longer demonstrate the surprising trend observed above when the lowest concentration was excluded (13.5% Adj. RSD neat *versus* 16.6% Adj. RSD matrix). Using the adjusted linearity metric, PRM was not significantly affected by the presence of matrix (or isolation width, as before) (supplemental Tables S4*G*, S4*H*).

QqQ SRM Measurement Precision, Dynamic Range, and Linearity—Like the PRM data described above, the QqQ SRM data, which queried a subset of 14 of the 25 peptides analyzed on the QqOrbi, also exhibited a high degree of run-to-run measurement precision, typically less than 15% RSD. Unlike in PRM, however, measurement precision, when all peptides and concentrations were considered together, was significantly greater in the presence of matrix (supplemental Table S5*A*). Lower peptide concentrations were again correlated with decreased measurement precision, though only significantly so under neat conditions (supplemental Table S5*B*). Peptides were quantified on average over concentration ranges of $10^{3.3}$ (neat) and $10^{2.2}$ (matrix), and the depression of dynamic range under matrix-containing conditions was statistically significant. Linearity under matrix conditions bested that under neat conditions with mean %RSDs of 16.7 and 42.1%, respectively. As in the QqOrbi, the loss of linearity was often the result of peptide detection at the lowest concentrations. Exclusion of these concentrations in %RSD calculations revealed no differences in linearity between matrix and neat conditions. Likewise, if only data covering the same dynamic range in both matrix-containing and neat conditions were considered, effectively truncating the neat data to the concentration range quantified in the matrix-containing data, linearity differences due to matrix interferences were not significant. Adjusted %RSDs, however, still exhibited significantly decreased linearity in the neat case. Mean adjusted %RSDs were 13.0 and 8.0% for neat and matrix data, respectively (supplemental Table S5*C*).

We postulate that the adjusted %RSD correction did not completely account for differences in linearity, as it did in the PRM data, because the SRM detection criteria were not sensitive enough to detect and exclude data at the lowest detected concentrations in neat experiments that were skewed by small amounts of chemical interference. In the matrix-containing SRM experiments, on the other hand, more abundant matrix interferences were easily detected and excluded by the detection criteria (supplemental Fig. S4). Detection criteria incorporating HR/AM data, however, more sensitively detected and excluded aberrant responses and thus, deviations in linearity were predictable and correctable (as adjusted %RSDs) based on the detected dynamic range. This same rationale can be applied to the discussion of measurement precision above: when all neat data were considered, precision was diminished relative to the matrix-containing data set because of the inclusion of background-skewed data not excluded by the detection criteria.

Empirical Comparison of QqQ SRM and QqOrbi PRM—To compare between QqQ SRM and QqOrbi PRM, we only considered the fourteen peptides analyzed in both data sets. Under neat conditions, run-to-run measurement precision (paired by peptide and concentration) was no different between QqQ SRM and QqOrbi PRM, regardless of the PRM isolation width employed. In the presence of matrix, however, SRM demonstrated significantly better measurement precision compared with both PRM data sets (5.6 *versus* 11.1% RSD, respectively; supplemental Tables S6*A*, S6*B*). Because neat SRM measurement precision, as discussed above, is believed to be artificially decreased because of the inclusion of chemical interference, it is likely that SRM exhibits superior measurement precision under neat conditions as well (supplemental Results and Discussion 2.3, Supplemental Table S6*B*).

SRM exhibited greater measurement precision likely because of the higher sampling rate of the QqQ (almost twice as many scans were acquired compared with the QqOrbi per 90 min chromatographic run). The ability of the QqQ to sample more points over a given chromatographic peak provided a more accurate determination of the peak AUC and, in turn, greater run-to-run repeatability. The difference in sampling rate between the two methods is due to the characteristics of the instruments used and, to some extent, necessary aspects of the experimental design. Because the QqQ is a "beam-type" instrument (as opposed to a scanning instrument like the QqOrbi), it operates at a duty cycle nearing 100%; this means that there is very little "down time" where the instru-

TABLE II
Comparison of QqQ SRM and QqOrbi PRM dynamic range and linearity

	SRM	PRM	
		±0.2 Th	±1 Th
Means			
Neat			
# orders	3.3	2.7	3.5
%RSD	42.09	29.99	27.36
$\%RSD_{adj}$	12.97	11.80	7.72
Matrix			
# orders	2.2	2.4	2.9
%RSD	16.09	29.98	29.08
$\%RSD_{adj}$	8.03	13.07	10.49
p values (SRM vs. PRM)			
Neat			
# orders		**2.61E-02**[b]	1.89E-01
%RSD		**2.33E-02**[a]	**8.74E-04**[a]
$\%RSD_{adj}$		2.38E-01	**1.99E-05**[a]
Matrix			
# orders		5.47E-01	**2.77E-03**[a]
%RSD		**2.72E-02**[b]	**3.08E-02**[b]
$\%RSD_{adj}$		1.05E-01	5.11E-01

[a] PRM data show significantly greater linearity or dynamic range (α = 5E-02).
[b] SRM data show significantly greater linearity or dynamic range (α = 5E-02).

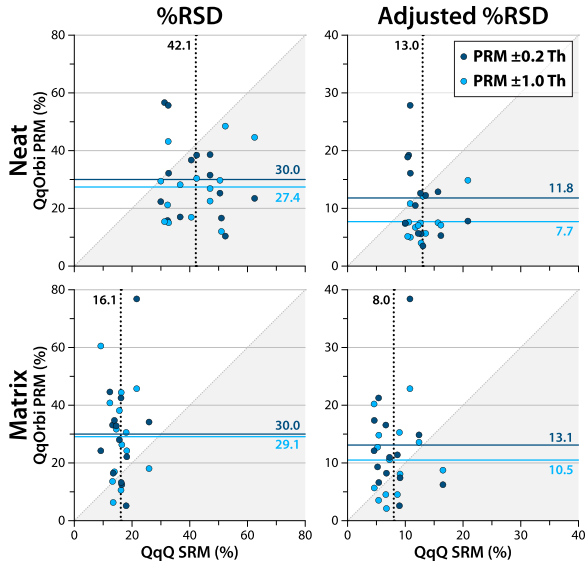

FIG. 4. **Comparison of linearity as %RSD and adjusted %RSD (supplemental Equation S1) for the 14 shared peptides targeted in QqOrbi PRM experiments (*y* axis) and QqQ SRM (*x* axis) under neat and matrix-containing conditions.** *Solid horizontal lines* and *dotted vertical lines* represent the mean %RSD value, also labeled in the plot, of the associated data set. Data falling in the *gray region* demonstrate greater linearity in PRM experiments. Data in the *white region* demonstrate greater linearity in SRM experiments.

ment is not acquiring data. The Orbitrap, conversely, as a scanning instrument, has inefficiencies inherent to its design. The Orbitrap transients employed here (required for MS/MS scans of resolution 17,500) were approximately twice the length of the 35 ms dwell times employed in the SRM method. Additionally, whereas the QqQ cycle time was fixed, the cycle time of the QqOrbi varied based on ion accumulation times, which were dynamically set based on ion flux. At low sample concentrations, QqOrbi injection times could reach as high as 120 ms to result in (at most) ~40 ms of inter-scan "down time" where mass analysis was not occurring. Shorter transients and lower maximum allowable injection times could be used to match the cycle times of the two methods at the expense of overall performance: shorter injection times would decrease spectral quality/usability when ion flux is low, and lower mass analysis resolution would undermine the benefits that high selectivity brings to the PRM method.

Greater QqQ SRM measurement precision did not translate into greater sensitivity or linearity compared with PRM. Under neat conditions, SRM quantified a concentration range spanning $10^{3.3}$ per peptide on average. This range is not statistically different from that achieved with PRM, $10^{3.5}$, at the wider isolation width. In matrix-containing experiments, however, PRM quantified over a broader range at both isolation widths ($10^{2.4}$ and $10^{2.9}$ at ±0.2 and ±1 Th, respectively) than did SRM ($10^{2.2}$), and significantly more at the ±1 Th isolation width (Table II). This result is illustrated on an individual peptide basis in Fig. 3*B*. For both neat and matrix containing experiments, the lowest concentration detected for each peptide studied in the SRM and PRM (±1 Th) experiments is plotted. SRM demonstrates a lower empirical detection limit than PRM in only one case (peptide NSWGTDWGEk, neat). As an aside, under matrix-containing conditions, SRM surprisingly performed no better QqOrbi SIM: SIM quantified on average over a range of $10^{2.0}$ at an isolation width ±1 Th, statistically no different from SRM (see supplemental Results and Discussion 2.5–2.6, supplemental Table S6*C*).

Under neat conditions, PRM demonstrated significantly higher linearity over the quantified dynamic range compared with QqQ SRM (Table II). Given that PRM under matrix-containing conditions yielded quantitative data over a wider dynamic range than SRM, we calculated adjusted %RSDs, as before, to normalize the linearity metric for the dynamic range detected and permit a fair comparison of the data. With this consideration, PRM linearity was statistically no different from the linearity exhibited by SRM (Table II). Fig. 4 plots the SRM linearity data for each of the targeted peptides as a function of PRM linearity and is stratified by the presence of matrix and isolation width. This data presentation demonstrates the effect of using the adjusted linearity metric on mean linearity estimates (shown as vertical and horizontal lines), as well as the relative distributions of the linearity metrics across the data sets.

With these data, we find that a high resolution and accurate mass MS can acquire data of similar quality to that collected on a QqQ in a targeted, quantitative proteomics context with 1) minimal upfront development time, 2) straightforward data analysis, and 3) similar performance metrics. Our PRM methods were designed and optimized on a method-level, rather

than on the peptide-level as with SRM methods (*i.e.* optimization of individual collision energies and transition sets for each target peptide). Thus, the PRM method has fewer parameters that require optimization (namely, only maximum injection time/AGC target, "global" collision energy, and, optionally, target scheduling) and can be performed with solely knowledge of the mass-to-charge ratios of the target peptides (and, optionally, the approximate retention time). These characteristics make PRM amenable to the "walk-up" instrument user who wishes to perform targeted, quantitative assays on a list of targets in a time-efficient manner—collection of MS/MS data and optimization of individual transition sets not required. We believe that the data presented here reflect the analytical performance a typical user might expect for PRM, however the analysis parameters used here may not represent the optimum conditions for all applications of PRM and would require application-specific investigation.

In addition to the minimal upfront method development needed to successfully perform a quantitative PRM assay, a notable aspect of using HR/AM data for targeted proteomics is the ease with which data can be interpreted and data analysis can be automated. Within the course of this study, we developed and automated a novel strategy for scoring and detecting low level analytes in complex, chimeric Orbitrap spectra that allowed sensitive detection of our target peptides without the expense of selectivity. The specificity of accurate mass measurements and the resulting paucity of marginal or ambiguous situations in the data (which are difficult to account for in automated methods) enabled this rather simple algorithm. On the other hand, even using well-established and optimized detection criteria from the literature for SRM, the SRM detection criteria were not sensitive enough to successfully detect and exclude data skewed by small amounts of chemical interference, leading to poor reproducibility and linearity. Furthermore, with the high specificity of a product ion measured at high mass accuracy for a target peptide (as demonstrated by our theoretical calculations) and the benefit of full mass-range mass analysis, the PRM paradigm lends itself well to future development of how targeted, quantitative proteomic data are analyzed. Through use of theoretical calculations, the high specificity of high mass accuracy data lays the groundwork for a generalized and statistically sound detection algorithm for reaction monitoring experiments that incorporates probability of correctness measures, as well as obviates the need for manual curation, *ad hoc* detection criteria (42), "decoy transitions" at the measurement-level (66), and the potentially high level of human intervention (and error) that comes with such detection strategies.

Last, our analysis of the analytical performance characteristics of PRM suggests that targeted HR/AM methods can rival the performance of QqQ SRM in terms of dynamic range, linearity, and, to a lesser extent, precision. Although SRM measurement precision was ~twofold better (under matrix-containing experiments) likely because of differences in scan rate between the two mass analyzers, PRM yielded quantitative data over a wider dynamic range than SRM under matrix-containing conditions. High mass accuracy and high resolution underlie this result: when high levels of matrix background are present, a single stage of isolation in combination with highly resolved data is statistically significantly more sensitive than two stages of isolation in combination with low resolution data, the "gold-standard" method for quantitative proteomic analyses. Additionally, achievable linearity over the quantifiable dynamic range was found to be statistically the same between SRM and PRM. Thus, in answer to the query posed in our theoretical comparison of SRM and PRM, our experimental data suggest that high selectivity/specificity can overcome limitations in speed and sensitivity to reliably provide lower detection limits and higher accuracy measurements. We conclude that the proposed PRM analysis paradigm holds promise as a viable, and accessible, alternative and/or complement to SRM for the quantitative proteomics toolbox.

In support of our conclusions, a report by Weisbrod *et al.* (61), published during the preparation of this manuscript, described a method for data-independent discovery proteomics on an Oribtrap MS that reinforces the favorable performance of PRM relative to SRM for targeted proteomics. In their "Fourier Transform-All Reaction Monitoring" (FT-ARM) method performed on a QLT-Orbitrap MS, wide swaths of mass-to-charge space (*i.e.* 100 Th) were accumulated and isolated in the QLT using broadband waveforms, subjected in bulk to dissociation, and simultaneously mass analyzed to exploit the HR/AM properties of the Orbitrap. The authors noted the ability to quantify peptides with FT-ARM, using the product ions generated from in-bulk dissociation, with modest sensitivity, reproducibility, and precision despite quite significant interferences from other ions present in the 100 Th isolation swath. This further corroborates that HR/AM mass analysis enables real, quantitative information to be extracted from highly interference-riddled measurements with little upfront assay development or optimization. Because PRM involves significantly less co-isolated interference and uses a quadrupole mass filter-equipped platform better suited to accumulation and isolation of large quantities of ions (to improve sensitivity), these findings further support our conclusions that PRM yields high quality quantitative measurements, comparable to QqQ SRM, while simplifying method development.

Looking forward, the PRM paradigm also enables new modes of analysis that are currently unavailable on QqQ platforms. Because of the modular nature of hybrid HR/AM MS, these platforms provide an unprecedented amount of experimental flexibility. Possessing the capabilities of both high performance quantitative and high-throughput discovery proteomics instruments, one can envision mixed mode analysis types in which targeted and discovery experiments are performed simultaneously. For example, when not engaged in

profiling an eluting target species, the instrument could be directed to perform conventional data-dependent or data-independent MS/MS, thereby maximizing instrument time, sample usage, and data density. Additionally, because of the high specificity of ions measured at high mass accuracy and consequently the reduced search space for potentially matching peptides, intelligent data acquisition strategies are possible that enable on-the-fly database searching, spectral matching, or spectral scoring (like that used here post-acquisition). Such strategies would enable the mass spectrometer to make decisions during acquisition, such as assessing whether a target peptide had been adequately identified, changing experimental parameters (CAD energies, isolation width, injection times, etc.) to improve performance for a particular target peptide, or determining its progress in a chromatographic run to make dynamic modifications to target peptide scheduling (67, 68).

Acknowledgments—We thank Alex Hebert for sample preparation and helpful discussions.

* This work was funded by the National Institutes of Health (R01GM080148) and National Science Foundation (CHE-0747990).

§ To whom correspondence should be addressed: 425 Henry Mall, Madison, WI 53706. Tel.: (608) 263-1718; E-mail: jcoon@chem.wisc.edu.

S This article contains supplemental Figs. S1 to S6, Tables S1 to S6 as well as Methods, Results and Discussion.

REFERENCES

1. Parker, C. E., Pearson, T. W., Anderson, N. L., and Borchers, C. H. (2010) Mass-spectrometry-based clinical proteomics - a review and prospective. *Analyst* **135,** 1830–1838
2. Kirkpatrick, D. S., Gerber, S. A., and Gygi, S. P. (2005) The absolute quantification strategy: a general procedure for the quantification of proteins and post-translational modifications. *Methods* **35,** 265–273
3. Phanstiel, D., Unwin, R., McAlister, G. C., and Coon, J. J. (2009) Peptide quantification using 8-plex isobaric tags and electron transfer dissociation tandem mass spectrometry. *Anal. Chem.* **81,** 1693–1698
4. Wu, C. C., MacCoss, M. J., Howell, K. E., Matthews, D. E., and Yates, J. R. (2004) Metabolic labeling of mammalian organisms with stable isotopes for quantitative proteomic analysis. *Anal. Chem.* **76,** 4951–4959
5. Ong, S. E., Blagoev, B., Kratchmarova, I., Kristensen, D. B., Steen, H., Pandey, A., and Mann, M. (2002) Stable isotope labeling by amino acids in cell culture, SILAC, as a simple and accurate approach to expression proteomics. *Mol. Cell. Proteomics* **1,** 376–386
6. Zhu, H., Pan, S., Gu, S., Bradbury, E. M., and Chen, X. (2002) Amino acid residue specific stable isotope labeling for quantitative proteomics. *Rapid Commun. Mass Spectrom.* **16,** 2115–2123
7. Mallick, P., and Kuster, B. (2010) Proteomics: a pragmatic perspective. *Nat. Biotechnol.* **28,** 695–709
8. Grossmann, J., Roschitzki, B., Panse, C., Fortes, C., Barkow-Oesterreicher, S., Rutishauser, D., and Schlapbach, R. (2010) Implementation and evaluation of relative and absolute quantification in shotgun proteomics with label-free methods. *J. Proteomics* **73,** 1740–1746
9. Matallana-Surget, S., Leroy, B., and Wattiez, R. (2010) Shotgun proteomics: concept, key points and data mining. *Expert Rev. Proteomics* **7,** 5–7
10. Wu, C. C., and MacCoss, M. J. (2002) Shotgun proteomics: Tools for the analysis of complex biological systems. *Curr. Opin Mol. Ther.* **4,** 242–250
11. Eng, J. K., McCormack, A. L., and Yates, J. R. (1994) An approach to correlate tandem mass spectral data of peptides with amino acid sequences in a protein database. *J. Am. Soc. Mass Spectrom.* **5,** 976–989
12. Perkins, D. N., Pappin, D. J., Creasy, D. M., and Cottrell, J. S. (1999) Probability-based protein identification by searching sequence databases using mass spectrometry data. *Electrophoresis* **20,** 3551–3567
13. Geer, L. Y., Markey, S. P., Kowalak, J. A., Wagner, L., Xu, M., Maynard, D. M., Yang, X., Shi, W., and Bryant, S. H. (2004) Open mass spectrometry search algorithm. *J Proteome Res* **3,** 958–964
14. Liu, H., Sadygov, R. G., and Yates, J. R. 3rd (2004) A model for random sampling and estimation of relative protein abundance in shotgun proteomics. *Anal. Chem.* **76,** 4193–4201
15. Tabb, D. L., Vega-Montoto, L., Rudnick, P. A., Variyath, A. M., Ham, A. J., Bunk, D. M., Kilpatrick, L. E., Billheimer, D. D., Blackman, R. K., Cardasis, H. L., Carr, S. A., Clauser, K. R., Jaffe, J. D., Kowalski, K. A., Neubert, T. A., Regnier, F. E., Schilling, B., Tegeler, T. J., Wang, M., Wang, P., Whiteaker, J. R., Zimmerman, L. J., Fisher, S. J., Gibson, B. W., Kinsinger, C. R., Mesri, M., Rodriguez, H., Stein, S. E., Tempst, P., Paulovich, A. G., Liebler, D. C., and Spiegelman, C. (2010) Repeatability and reproducibility in proteomic identifications by liquid chromatography-tandem mass spectrometry. *J. Proteome Res.* **9,** 761–776
16. Gupta, M. K., Jung, J. W., Uhm, S. J., Lee, H., Lee, H. T., and Kim, K. P. (2009) Combining selected reaction monitoring with discovery proteomics in limited biological samples. *Proteomics* **9,** 4834–4836
17. Yang, X., and Lazar, I. M. (2009) MRM screening/biomarker discovery with linear ion trap MS: a library of human cancer-specific peptides. *BMC Cancer* **9,** 96
18. Schmidt, A., Gehlenborg, N., Bodenmiller, B., Mueller, L. N., Campbell, D., Mueller, M., Aebersold, R., and Domon, B. (2008) An integrated, directed mass spectrometric approach for in-depth characterization of complex peptide mixtures. *Mol. Cell. Proteomics* **7,** 2138–2150
19. Schmidt, A., Claassen, M., and Aebersold, R. (2009) Directed mass spectrometry: towards hypothesis-driven proteomics. *Curr. Opin. Chem. Biol.* **13,** 510–517
20. Addona, T. A., Abbatiello, S. E., Schilling, B., Skates, S. J., Mani, D. R., Bunk, D. M., Spiegelman, C. H., Zimmerman, L. J., Ham, A. J., Keshishian, H., Hall, S. C., Allen, S., Blackman, R. K., Borchers, C. H., Buck, C., Cardasis, H. L., Cusack, M. P., Dodder, N. G., Gibson, B. W., Held, J. M., Hiltke, T., Jackson, A., Johansen, E. B., Kinsinger, C. R., Li, J., Mesri, M., Neubert, T. A., Niles, R. K., Pulsipher, T. C., Ransohoff, D., Rodriguez, H., Rudnick, P. A., Smith, D., Tabb, D. L., Tegeler, T. J., Variyath, A. M., Vega-Montoto, L. J., Wahlander, A., Waldemarson, S., Wang, M., Whiteaker, J. R., Zhao, L., Anderson, N. L., Fisher, S. J., Liebler, D. C., Paulovich, A. G., Regnier, F. E., Tempst, P., and Carr, S. A. (2009) Multi-site assessment of the precision and reproducibility of multiple reaction monitoring-based measurements of proteins in plasma. *Nat. Biotechnol.* **27,** 633–641
21. Lange, V., Picotti, P., Domon, B., and Aebersold, R. (2008) Selected reaction monitoring for quantitative proteomics: a tutorial. *Mol. Syst. Biol.* **4,** 10.1038/msb.2008.61
22. Anderson, N. L., Anderson, N. G., Pearson, T. W., Borchers, C. H., Paulovich, A. G., Patterson, S. D., Gillette, M., Aebersold, R., and Carr, S. A. (2009) A human proteome detection and quantitation project. *Mol. Cell. Proteomics* **8,** 883–886
23. Keshishian, H., Addona, T., Burgess, M., Kuhn, E., and Carr, S. A. (2007) Quantitative, multiplexed assays for low abundance proteins in plasma by targeted mass spectrometry and stable isotope dilution. *Mol. Cell. Proteomics* **6,** 2212–2229
24. Kuzyk, M. A., Smith, D., Yang, J., Cross, T. J., Jackson, A. M., Hardie, D. B., Anderson, N. L., and Borchers, C. H. (2009) Multiple reaction monitoring-based, multiplexed, absolute quantitation of 45 proteins in human plasma. *Mol. Cell. Proteomics* **8,** 1860–1877
25. Whiteaker, J. R., Lin, C., Kennedy, J., Hou, L., Trute, M., Sokal, I., Yan, P., Schoenherr, R. M., Zhao, L., Voytovich, U. J., Kelly-Spratt, K. S., Krasnoselsky, A., Gafken, P. R., Hogan, J. M., Jones, L. A., Wang, P., Amon, L., Chodosh, L. A., Nelson, P. S., McIntosh, M. W., Kemp, C. J., and Paulovich, A. G. (2011) A targeted proteomics-based pipeline for verification of biomarkers in plasma. *Nat. Biotechnol.* **29,** 625–634
26. Pan, S., Chen, R., Brand, R. E., Hawley, S., Tamura, Y., Gafken, P. R., Milless, B. P., Goodlett, D. R., Rush, J., and Brentnall, T. A. (2012) Multiplex targeted proteomic assay for biomarker detection in plasma: a pancreatic cancer biomarker case study. *J. Proteome Res.* **11,** 1937–1948
27. Anderson, L., and Hunter, C. L. (2006) Quantitative mass spectrometric multiple reaction monitoring assays for major plasma proteins. *Mol. Cell. Proteomics* **5,** 573–588
28. Costenoble, R., Picotti, P., Reiter, L., Stallmach, R., Heinemann, M., Sauer,

U., and Aebersold, R. (2011) Comprehensive quantitative analysis of central carbon and amino-acid metabolism in Saccharomyces cerevisiae under multiple conditions by targeted proteomics. *Mol. Syst. Biol.* **7,** 10.1038/msb.2010.122
29. Picotti, P., Bodenmiller, B., Mueller, L. N., Domon, B., and Aebersold, R. (2009) Full Dynamic Range Proteome Analysis of S. cerevisiae by Targeted Proteomics. *Cell* **138,** 795–806
30. Agard, N. J., Mahrus, S., Trinidad, J. C., Lynn, A., Burlingame, A. L., and Wells, J. A. (2012) Global kinetic analysis of proteolysis via quantitative targeted proteomics. *Proc. Natl. Acad. Sci. U.S.A.* **109,** 1913–1918
31. Mallick, P., Schirle, M., Chen, S. S., Flory, M. R., Lee, H., Martin, D., Ranish, J., Raught, B., Schmitt, R., Werner, T., Kuster, B., and Aebersold, R. (2007) Computational prediction of proteotypic peptides for quantitative proteomics. *Nat. Biotechnol.* **25,** 125–131
32. Cham Mead, J. A., Bianco, L., and Bessant, C. (2010) Free computational resources for designing selected reaction monitoring transitions. *Proteomics* **10,** 1106–1126
33. Prakash, A., Tomazela, D. M., Frewen, B., MacLean, B., Merrihew, G., Peterman, S., and MacCoss, M. J. (2009) Expediting the Development of Targeted SRM Assays: Using Data from Shotgun Proteomics to Automate Method Development. *J. Proteome Res.* **8,** 2733–2739
34. Deutsch, E. W., Lam, H., and Aebersold, R. (2008) PeptideAtlas: a resource for target selection for emerging targeted proteomics workflows. *EMBO Rep.* **9,** 429–434
35. Craig, R., Cortens, J. P., and Beavis, R. C. (2004) Open source system for analyzing, validating, and storing protein identification data. *J. Proteome Res.* **3,** 1234–1242
36. Siepen, J. A., Belhajjame, K., Selley, J. N., Embury, S. M., Paton, N. W., Goble, C. A., Oliver, S. G., Stevens, R., Zamboulis, L., Martin, N., Poulovassillis, A., Jones, P., Cote, R., Hermjakob, H., Pentony, M.M., Jones, D. T., Orengo, C. A., and Hubbard, S. J. (2008) ISPIDER Central: an integrated database web-server for proteomics. *Nucleic Acids Res.* **36,** W485–W490
37. Jones, P., Côté, R. G., Cho, S.Y., Klie, S., Martens, L., Quinn, A. F., Thorneycroft, D., and Hermjakob, H. (2008) PRIDE: new developments and new datasets. *Nucleic Acids Res.* **36,** D878–D883
38. Desiere, F., Deutsch, E. W., King, N. L., Nesvizhskii, A. I., Mallick, P., Eng, J., Chen, S., Eddes, J., Loevenich, S. N., and Aebersold, R. (2006) The PeptideAtlas project. *Nucleic Acids Res.* **34,** D655–D658
39. Mathivanan, S., Ahmed, M., Ahn, N. G., Hainard, A., Amanchy, R., Andrews, P. C., Bader, J. S., Balgley, B. M., Bantscheff, M., Bennett, K. L., Bjorling, E., Blagoev, B., Bose, R., Brahmachari, S. K., Burlingame, A. S., Bustelo, X. R., Cagney, G., Cantin, G. T., Cardasis, H. L., Celis, J. E., Chaerkady, R., Chu, F. X., Cole, P. A., Costello, C. E., Cotter, R. J., Crockett, D., DeLany, J. P., De Marzo, A. M., DeSouza, L. V., Deutsch, E. W., Dransfield, E., Drewes, G., Droit, A., Dunn, M. J., Elenitoba-Johnson, K., Ewing, R. M., Van Eyk, J., Faca, V., Falkner, J., Fang, X. M., Fenselau, C., Figeys, D., Gagne, P., Gelfi, C., Gevaert, K., Gimble, J. M., Gnad, F., Goel, R., Gromov, P., Hanash, S. M., Hancock, W. S., Harsha, H. C., Hart, G., Hays, F., He, F. C., Hebbar, P., Helsens, K., Hermeking, H., Hide, W., Hjerno, K., Hochstrasser, D. F., Hofmann, O., Horn, D. M., Hruban, R. H., Ibarrola, N., James, P., Jensen, O. N., Jensen, P. H., Jung, P., Kandasamy, K., Kheterpal, I., Kikuno, R. F., Korf, U., Korner, R., Kuster, B., Kwon, M. S., Lee, H. J., Lee, Y. J., Lefevre, M., Lehvaslaiho, M., Lescuyer, P., Levander, F., Lim, M. S., Lobke, C., Loo, J. A., Mann, M., Martens, L., Martinez-Heredia, J., McComb, M., McRedmond, J., Mehrle, A., Menon, R., Miller, C. A., Mischak, H., Mohan, S. S., Mohmood, R., Molina, H., Moran, M. F., Morgan, J. D., Moritz, R., Morzel, M., Muddiman, D. C., Nalli, A., Navarro, J. D., Neubert, T. A., Ohara, O., Oliva, R., Omenn, G. S., Oyama, M., Paik, Y. K., Pennington, K., Pepperkok, R., Periaswamy, B., Petricoin, E. F., Poirier, G. G., Prasad, T. S., Purvine, S. O., Rahiman, B. A., Ramachandran, P., Ramachandra, Y. L., Rice, R. H., Rick, J., Ronnholm, R. H., Salonen, J., Sanchez, J. C., Sayd, T., Seshi, B., Shankari, K., Sheng, S. J., Shetty, V., Shivakumar, K., Simpson, R. J., Sirdeshmukh, R., Siu, K. W., Smith, J. C., Smith, R. D., States, D. J., Sugano, S., Sullivan, M., Superti-Furga, G., Takatalo, M., Thongboonkerd, V., Trinidad, J. C., Uhlen, M., Vandekerckhove, J., Vasilescu, J., Veenstra, T. D., Vidal-Taboada, J. M., Vihinen, M., Wait, R., Wang, X., Wiemann, S., Wu, B., Xu, T., Yates, J. R., Zhong, J., Zhou, M., Zhu, Y., Zurbig, P., and Pandey, A. (2008) Human Proteinpedia enables sharing of human protein data. *Nat. Biotechnol.* **26,** 164–167
40. Picotti, P., Lam, H., Campbell, D., Deutsch, E. W., Mirzaei, H., Ranish, J., Domon, B., and Aebersold, R. (2008) A database of mass spectrometric assays for the yeast proteome. *Nat. Methods* **5,** 913–914
41. Farrah, T., Deutsch, E.W., Kreisberg, R., Sun, Z., Campbell, D.S., Mendoza, L., Kusebauch, U., Brusniak, M.-Y., Hüttenhain, R., Schiess, R., Selevsek, N., Aebersold, R., and Moritz, R.L. (2012) PASSEL: The PeptideAtlas SRM Experiment Library. *Proteomics* **12,** 10.1002/pmic.201100515
42. Picotti, P., Rinner, O., Stallmach, R., Dautel, F., Farrah, T., Domon, B., Wenschuh, H., and Aebersold, R. (2010) High-throughput generation of selected reaction-monitoring assays for proteins and proteomes. *Nat. Methods* **7,** 43–46
43. Kiyonami, R., Schoen, A., Prakash, A., Peterman, S., Zabrouskov, V., Picotti, P., Aebersold, R., Huhmer, A., and Domon, B. (2011) Increased selectivity, analytical precision, and throughput in targeted proteomics. *Mol. Cell. Proteomics* **10,** 10.1074/mcp.M110.002931
44. Mann, M., and Kelleher, N. L. (2008) Precision proteomics: the case for high resolution and high mass accuracy. *Proc. Natl. Acad. Sci. U.S.A.* **105,** 18132–18138
45. Andrews, G. L., Simons, B. L., Young, J. B., Hawkridge, A. M., and Muddiman, D. C. (2011) Performance characteristics of a new hybrid quadrupole time-of-flight tandem mass spectrometer (TripleTOF 5600). *Anal. Chem.* **83,** 5442–5446
46. Hu, Q., Noll, R. J., Li, H., Makarov, A., Hardman, M., and Cooks, R. G. (2005) The Orbitrap: a new mass spectrometer. *J. Mass Spectrom.* **40,** 430–443
47. Michalski, A., Damoc, E., Hauschild, J. P., Lange, O., Wieghaus, A., Makarov, A., Nagaraj, N., Cox, J., Mann, M., and Horning, S. (2011) Mass spectrometry-based proteomics using Q Exactive, a high-performance benchtop quadrupole Orbitrap mass spectrometer. *Mol. Cell. Proteomics* **10,** 10.1074/mcp.M111.011015
48. Michalski, A., Damoc, E., Lange, O., Denisov, E., Nolting, D., Mueller, M., Viner, R., Schwartz, J., Remes, P., Belford, M., Dunyach, J. J., Cox, J., Horning, S., Mann, M., and Makarov, A. (2012) Ultra high resolution linear ion trap Orbitrap mass spectrometer (Orbitrap Elite) facilitates top down LC MS/MS and versatile peptide fragmentation modes. *Mol. Cell. Proteomics* **11,** 10.1074/mcp.O111.013698
49. Olsen, J. V., Schwartz, J. C., Griep-Raming, J., Nielsen, M. L., Damoc, E., Denisov, E., Lange, O., Remes, P., Taylor, D., Splendore, M., Wouters, E. R., Senko, M., Makarov, A., Mann, M., and Horning, S. (2009) A dual pressure linear ion trap Orbitrap instrument with very high sequencing speed. *Mol. Cell. Proteomics* **8,** 2759–2769
50. Lange, O., Makarov, A., Denisov, E., and Balschun, W. (2010) Accelerating spectral acquistion rate of Orbitrap mass spectrometry. In, 58th Conf Amer Soc Mass Spectrom. Salt Lake City, Utah
51. Zhang, Y., Hao, Z., Kellmann, M., and Huhmer, A. (2012) HR/AM targeted peptide quantitation on a Q Exactive MS: A unique combination of high selectivity, sensitivity, and throughput. Thermo Fisher Scientific (San Jose, CA) Application Note: 554
52. Makarov, A., Denisov, E., and Lange, O. (2009) Performance Evaluation of a High-field Orbitrap Mass Analyzer. *J. Am. Soc. Mass Spectrom.* **20,** 1391–1396
53. Nagaraj, N., Alexander Kulak, N., Cox, J., Neuhauser, N., Mayr, K., Hoerning, O., Vorm, O., and Mann, M. (2012) System-wide Perturbation Analysis with Nearly Complete Coverage of the Yeast Proteome by Single-shot Ultra HPLC Runs on a Bench Top Orbitrap. *Mol. Cell. Proteomics* **11,** 10.1074/mcp.M111.013722
54. Olsen, J. V., de Godoy, L. M. F., Li, G. Q., Macek, B., Mortensen, P., Pesch, R., Makarov, A., Lange, O., Horning, S., and Mann, M. (2005) Parts per million mass accuracy on an orbitrap mass spectrometer via lock mass injection into a C-trap. *Mol. Cell. Proteomics* **4,** 2010–2021
55. Haas, W., Faherty, B. K., Gerber, S. A., Elias, J. E., Beausoleil, S. A., Bakalarski, C. E., Li, X., Villén, J., and Gygi, S. P. (2006) Optimization and use of peptide mass measurement accuracy in shotgun proteomics. *Mol. Cell. Proteomics* **5,** 1326–1337
56. Roth, M. J., Forbes, A. J., Boyne, M. T., Kim, Y. B., Robinson, D. E., and Kelleher, N. L. (2005) Precise and parallel characterization of coding polymorphisms, alternative splicing, and modifications in human proteins by mass spectrometry. *Mol. Cell. Proteomics* **4,** 1002–1008
57. Sherman, J., McKay, M. J., Ashman, K., and Molloy, M. P. (2009) How specific is my SRM?: The issue of precursor and product ion redun-

dancy. *Proteomics* **9,** 1120–1123
58. Duncan, M. W., Yergey, A. L., and Patterson, S. D. (2009) Quantifying proteins by mass spectrometry: The selectivity of SRM is only part of the problem. *Proteomics* **9,** 1124–1127
59. Lee, M. V., Topper, S. E., Hubler, S. L., Hose, J., Wenger, C. D., Coon, J. J., and Gasch, A. P. (2011) A dynamic model of proteome changes reveals new roles for transcript alteration in yeast. *Mol. Syst. Biol.* **7,** 10.1038/msb.2011.48
60. Ficarro, S. B., Zhang, Y., Lu, Y., Moghimi, A. R., Askenazi, M., Hyatt, E., Smith, E. D., Boyer, L., Schlaeger, T. M., Luckey, C. J., and Marto, J. A. (2009) Improved electrospray ionization efficiency compensates for diminished chromatographic resolution and enables proteomics analysis of tyrosine signaling in embryonic stem cells. *Anal. Chem.* **81,** 3440–3447
61. Weisbrod, C. R., Eng, J. K., Hoopmann, M. R., Baker, T., and Bruce, J. E. (2012) Accurate Peptide fragment mass analysis: multiplexed Peptide identification and quantification. *J. Proteome Res.* **11,** 1621–1632
62. Ono, M., Shitashige, M., Honda, K., Isobe, T., Kuwabara, H., Matsuzuki, H., Hirohashi, S., and Yamada, T. (2006) Label-free quantitative proteomics using large peptide data sets generated by nanoflow liquid chromatography and mass spectrometry. *Mol. Cell. Proteomics* **5,** 1338–1347
63. Wang, G., Wu, W. W., Zeng, W., Chou, C. L., and Shen, R. F. (2006) Label-free protein quantification using LC-coupled ion trap or FT mass spectrometry: Reproducibility, linearity, and application with complex proteomes. *J. Proteome Res.* **5,** 1214–1223
64. Wang, W., Zhou, H., Lin, H., Roy, S., Shaler, T. A., Hill, L. R., Norton, S., Kumar, P., Anderle, M., and Becker, C. H. (2003) Quantification of Proteins and Metabolites by Mass Spectrometry without Isotopic Labeling or Spiked Standards. *Anal. Chem.* **75,** 4818–4826
65. Li, X. J., Yi, E. C., Kemp, C. J., Zhang, H., and Aebersold, R. (2005) A Software Suite for the Generation and Comparison of Peptide Arrays from Sets of Data Collected by Liquid Chromatography-Mass Spectrometry. *Mol. Cell. Proteomics* **4,** 1328–1340
66. Reiter, L., Rinner, O., Picotti, P., Huttenhain, R., Beck, M., Brusniak, M. Y., Hengartner, M. O., and Aebersold, R. (2011) mProphet: automated data processing and statistical validation for large-scale SRM experiments. *Nat. Methods* **8,** 430–435
67. Graumann, J., Scheltema, R. A., Zhang, Y., Cox, J., and Mann, M. (2012) A Framework for Intelligent Data Acquisition and Real-Time Database Searching for Shotgun Proteomics. *Mol. Cell. Proteomics* **11,** 10.1074/mcp.M111.013185
68. Bailey, D. J., Rose, C. M., McAlister, G. C., Brumbaugh, J., Yu, P., Wenger, C. D., Westphall, M. S., Thomson, J. A., and Coon, J. J. (2012) Instant spectral assignment for advanced decision tree-driven mass spectrometry. *Proc. Natl. Acad. Sci. U.S.A.* **109,** 8411–8416